Journal of Ceramic Processing Research. Vol. 21, No. 1, pp. 86~91 (2020)
(Received 29 September 2019, Received in revised form 18 November 2019, Accepted 9 December 2019)
https://doi.org/10.36410/jcpr.2020.21.1.86

J O U R N A L O F
Ceramic Processing Research

Effect of CeO_2 addition on crystallization and thermo-physical properties of Li_2O-ZnO-SiO_2 glass-ceramics

Ruixue Li, Qian Zhang, Xingliang Peng and Weizhen Liu*
Faculty of Resources and Environmental Engineering, Jiangxi University of Science and Technology, Ganzhou 341000,China

The effect of CeO_2 addition on crystallization and thermo-physical properties of lithium zinc silicate (LZS) glasses containing Li_2O-ZnO-SiO_2-Al_2O_3-Na_2O-P_2O_5 was investigated. The changes of CeO_2 contents (2-8 wt.%) had an obvious influence on the transition temperatures (T_g) and crystallization temperatures (T_c) of LZS glass-ceramics, and they increased with CeO_2 content increasing. According to XRD analysis, CeO_2 promoted the formation of cristobalite and β-spodumene crystals, and β-spodumene increased obviously. As the CeO_2 content increasing, the microstructure and microhardness (being 6.88 Gpa at 880 °C) of glass-ceramics had great changes. The average thermal expansion coefficient (20 - 450 °C) showed first increasing then decreasing, having a wide range. The maximum of thermal expansion coefficient was obtained when the glass-ceramics contained 4 wt.% CeO_2, being 175×10^{-7} K^{-1} (at 700 °C) and 178×10^{-7} K^{-1} (at 880 °C) respectively. Excellent thermo-physical properties indicate the glass has greater potential application, such as being used as sealing glass.

Keywords: Lithum zinc silicate, Crystallization, Thermal expansion coefficient, Microhardness.

Introduction

Currently there has been a considerable amount of interest on crystallization behavior and thermo-physical property of Li_2O-ZnO-SiO_2 glass-ceramics [1-7] due to their beneficial performances, e.g., a wide range of thermal expansion coefficient ($\alpha = 50 - 200 \times 10^{-7}$ K^{-1}) by controlling heat treatments and adding different elements, high electrical resistivity and good chemical durability. McMillan and Partridge in 1963 [8] first reported lithium zinc silicate glass-ceramics containing high proportions of zinc oxide. Later, they found glass-ceramics could also be employed to produce superior glass-ceramic-to-metal seals [9]. Donald *et al*. [10] studied a number of Li_2O-ZnO-SiO_2 materials containing relatively high concentrations of ZnO, including the influence of nucleating species and concentration, and an assessment of the thermal expansion characteristics and mechanical properties. And they summarized recent developments of glass-ceramic-to-metal seals and coatings to gain a better understanding of diffusion and reaction behavior of individual metallic [11]. The glass-ceramics are suitable for matching sealing to lots of metals and alloys with different thermal expansion coefficients such as copper alloys, nickel-based alloys, Fe-Ni-C alloys and stainless steel etc. It is generally agreed that the properties of glass-ceramics are dependent on the crystal contents, phases and their microstructure. Chemical compositions of basic glasses play very important roles in the formation of crystals. The crystallization characteristic of glass-ceramics is usually influenced markedly by adding some specific elements, such as rare earth elements. Recently, Y_2O_3, Nd_2O_3, Fe_2O_3, B_2O_3, CuO, alkali oxides and alkali earth oxides also have been used as flux in some glass-ceramics to study the changes of their crystallization and thermo-physical properties [12-19].

Cerium oxide, as a rare earth oxide flux, has been reported in many glass-ceramics studies. In some studies, it is used as raw material in glasses [20-24]. Mostly CeO_2 is used as additive to regulate the properties of glass-ceramics [25-27]. Sohn *et al*. [28] found that CeO_2 as a flux markedly decreased viscosity in MgO-Al_2O_3-SiO_2 glasses, and had a little influence on thermal expansion, mechanical properties and chemical durability of glasses. Anmin Hu *et al*. [29] investigated phase transformations of Li_2O-Al_2O_3-SiO_2 glasses with CeO_2 addition, and showed that the transformations of glass to *β*-quartz and of *β*-quartz to *β*-spodumene were accelerated by addition of CeO_2. Temuujin *et al*. [30] studied the influence of CeO_2 addition in crystallization behavior and mechanical properties of glass ceramics in the Na_2O-CaO-Al_2O_3-SiO_2 system, and found that CeO_2 added to glass ceramics enhanced hardness because of an increased crystal size. Yongsheng *et al*. [31] also found CeO_2 could improve the integrity of the glass network structure and enhance fracture toughness in CaO-Al_2O_3-SiO_2 system. In the previous research, we know CeO_2 in different glass systems has various influences on thermo-physical and mechanical properties. Therefore, in order to enhance the properties of lithium

*Corresponding author:
Tel : +8607978312071
Fax: +8607978312051
E-mail: 9120170002@jxust.edu.cn

zinc silicate (LZS) glass, it is essential to investigate the effect of CeO_2 on LZS glass.

The purpose of this research was to investigate the effect of different content of CeO_2 addition on crystallization and thermo-physical properties of Li_2O-ZnO-SiO_2 glasses. After leaning its effect on the properties, we could adjust them by adding different content of CeO_2 to make the glass-ceramic better seal to various metals.

Experimental Procedure

Composition and preparation of the glass

The chemical compositions (wt.%) of the glasses were given in Table 1. We used the ingredients SiO_2, ZnO, Li_2O and Na_2O. P_2O_5 was used as nucleating agent. The starting materials were SiO_2 (≥99.0%), ZnO (≥99.0%), Li_2CO_3 (≥97.0%), Na_2CO_3 (≥99.8%), $NH_4H_2PO_4$ (≥99.0%) and CeO_2 (≥99.0%). The weighted errors of all raw materials were controlled in the range of ±0.01 g.

Glasses were prepared by fusing regent-grade chemicals in a platinum crucible. The glass samples were melted and maintained at 1,400 ºC in an electric furnace for 3 h. The molten glasses were then poured into a preheated (480 ºC) graphite mould and immediately transferred to an annealing furnace set at 480 ºC, being held for 2 h for annealing before cooling down to room temperature. The transparent and bubble-free glasses were obtained. Based on the DSC curves, we made the nucleation temperature and crystallization temperature to obtain glass-ceramics.

Analytical methods

Differential scanning calorimeter (DSC, Netzsch 404PC, Germany) was used to determine the glass transition temperature (T_g) and crystallization temperature (T_c) of the glass samples. The DSC measurements were performed using ~15 mg of powdered samples (45-53 μm), which were placed in an alumina crucible. The temperature range of the samples was between 20 and 1,000 ºC at heating rate of 10 K/min. The measurement error was ±2 ºC.

X-ray diffraction (XRD, D/max, 2500 model, Rigaku, Japan) was used to investigate the crystalline phases of the samples. The diffractmeter was with Cu Kα radiation in the 2θ range from 10º to 80º at 0.02 steps, which operated at 40 kV and 50 mA at a scanning rate of 4 º/min. The crystalline phases were identified by matching the peak positions of the intense peaks with PCPDF standard cards.

The microstructure of glass-ceramics samples were examined by the scanning electron microscope (SEM, FEI Quanta-200, America). The samples were polished to under 1μm and eroded by HF (4 wt.%) for 60 s, then transferred them to an ultrasonic cleaning equipment for 1 h to eliminate impurities that did not dissolve in the acid before being sputtered with a gold coating. Crystal morphology could be observed clearly.

Vickers hardness (H_v) tests were tested on polished glass-ceramics samples, using a Matsuzawa microhardness tester (HVS-1000) with a pyramid shaped diamond indenter, applying loads 1.96 N for 30 s. At least 10 different positions measurements were taken for each sample to take the average values. Indentation diagonals were measured to calculate hardness values in GPa.

The thermal expansion coefficient (TEC) measurements were carried out in a thermo-mechanical analyzer (Netzsch DIL 402EP, Germany) in the temperature range 20-450 ºC at heating rate of 2 K/min, using a silica probe in an inert atmosphere using argon (50 ml/min). The samples were machined into 3 mm × 3 mm × 20 mm cuboid test bars. The average thermal expansion coefficient values were calculated in the temperature range of 20-450 ºC.

Table 1. Chemical compositions of the base glasses (± 0.02 wt.%)[a].

Glass code	Li_2O	ZnO	SiO_2	Al_2O_3	Na_2O	P_2O_5	CeO_2
C_0	9.00	22.00	57.00	5.00	4.00	3.00	0.00
C_2	8.82	21.56	55.86	4.90	3.92	2.94	2.00
C_4	8.64	21.12	54.72	4.80	3.84	2.88	4.00
C_6	8.46	20.68	53.58	4.70	3.76	2.82	6.00
C_8	8.28	20.24	52.44	4.60	3.68	2.76	8.00

[a]The error was caused by converting the content of oxide into that of raw material, weighting of raw materials, volatilizing of oxides and corroding on crucible surface

Results and Discussion

Crystalline phases and microstructure

Fig. 1 shows the DSC curves obtained from as-cast LZS glasses. There were obviously endothermic valleys on the differential thermal curves. The start points of the endothermic valleys (T_g, marked temperatures in Fig. 1) were from 485 to 510 ºC with CeO_2 content increasing. It indicated the glass transition temperature

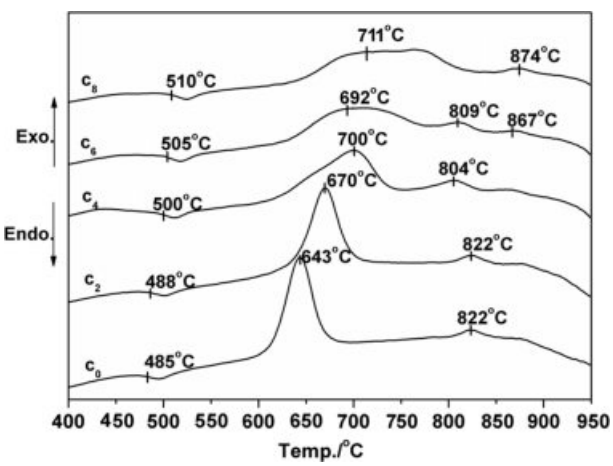

Fig. 1. DSC curves of the glass with different amounts of CeO_2.

Table 2. Characteristic temperature of glass specimens (± 2 ºC).

Glass code	T_g	T_{p1}	T_{p2}	T_{p3}	T_{p4}
C_0	485	643	-	822	-
C_2	488	670	-	822	-
C_4	500	700	804	-	-
C_6	505	692	809	-	867
C_8	510	711	-	-	874

(T_g) increased. Exothermic peaks were also obvious on the curves, and the peaks had changed. The temperatures of first peaks increased but the peak intensity (height and area) weakened at the same time. Crystallization peaks correspond to the formation of different crystalline phases. The curve shape of C_0 is similar with that of C_2, it showed that low content (under 2 wt.%) of CeO_2 would not have obvious influence on crystalline phases. As the CeO_2 content increasing, when it was above 4 wt.%, it had a bigger impact on the formation of crystals. The curves of C_4 and C_6 showed new peaks at 804 ºC and 809 ºC, and C_6 and C_8 both appeared another peaks at 867 ºC and 874 ºC. Table 2 given a summary of the results of differential scanning calorimetry: glass transition temperatures (T_g) and the peak temperatures of crystallization (T_p). The main crystals of LZS are lithium zinc silicate and cistobalite, and the formation temperatures of them are about 650 ºC and 750 ºC [34]. However, β-spodumene crystal formation temperature is about 850 ºC. According to the DSC curves, CeO_2 might promote the formation of new phase β-spodumene. On account of the analysis of DSC curves above, the nucleation temperature of the samples was set at 520 ºC for 2 h, and the crystallization temperatures were set at 700, 830 and 880 ºC for 2 h, respectively, to obtain glass-ceramics. We could know the crystal growth process from X-ray diffraction patterns.

Fig. 2 and 3 show the X-ray diffraction patterns of LZS glass-ceramics at different crystallization temperatures (700 ºC and 880 ºC). Fig. 2 shows the XRD patterns of the samples containing different amounts of CeO_2 crystallized at 700 ºC. Crystallization consequence of the CeO_2-free sample is quite simple, as C_0 showing. The major phases were Li_2ZnSiO_4 (PDF# 24-0677) and $Li_3Zn_{0.5}SiO_4$ (PDF# 24-0667), which was the same to LZS system. The curves of C_0, C_2 and C_4 in Fig. 2 are similar. It means that low content of CeO_2 (under 4 wt.%) in LZS system would not have obvious effect on the main crystals in the glass-ceramics at low crystallization temperature (700 ºC). However, the amounts of main crystals increased with CeO_2 content increasing. When CeO_2 content was over 6 wt.%, β-spodumene (PDF# 35-0797) appeared, which could be observed from C_6 and C_8 curves in Fig. 2. According to the XRD analysis result in Fig. 2, the Li_2ZnSiO_4 and $Li_3Zn_{0.5}SiO_4$ crystals were promoted by CeO_2, and the amount of cristobalite (PDF# 39-1425) also increased. High content of CeO_2 (above 6 wt.%) could accelerate crystals growth, especially for β-spodumene.

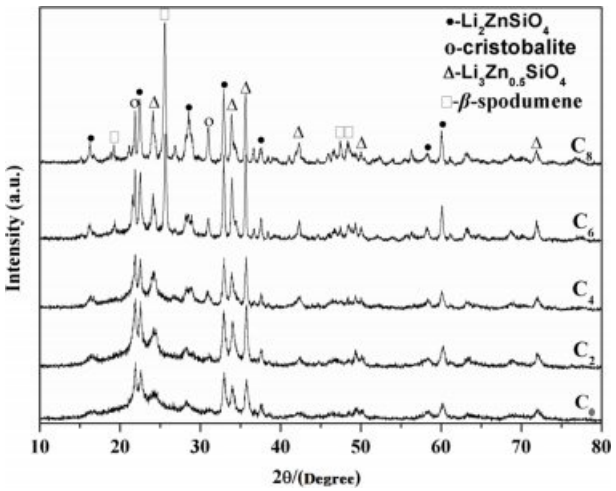

Fig. 2. X-ray diffraction patterns of the present glasses heat-treated at 700 ºC for 2 h.

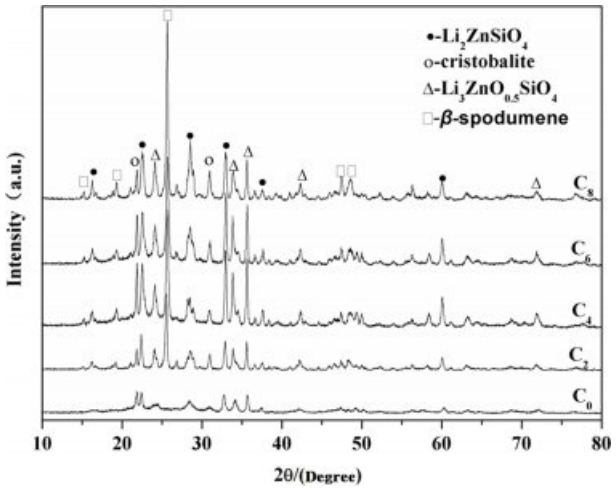

Fig. 3. X-ray diffraction patterns of the present glasses heat-treated at 880 ºC for 2 h.

Fig. 3 shows the XRD patterns for the samples crystallized at 880 ºC. Li_2ZnSiO_4 and $Li_3Zn_{0.5}SiO_4$ also were identified as major crystallization phases along with cristobalite phase increasing when the amount of CeO_2 was under 2 wt.%, according to C_0 and C_2 curves in Fig. 3. C_0 curve in Fig. 3 had no obvious difference with C_0 in Fig. 2, but at 880 ºC, C_2 appeared β-spodumene, and cristobalite increased. It indicated that temperature also had a distinct effect on the formation of β-spodumene and cristobalite. At high crystallization temperature (880 ºC), CeO_2 could better promote crystals growth. The CeO_2-free samples had no β-spodumene phase, regardless of temperature. The amounts of Li_2ZnSiO_4, $Li_3Zn_{0.5}SiO_4$ and cristobalite also increased as CeO_2 increasing at 880 ºC. The samples containing high amount of CeO_2 (6 wt.%) at low crystallization temperature (700 ºC) had the same crystalline phases with the samples containing low amount of CeO_2 (2 wt.%) at

high crystallization temperature (880 °C). When the content of CeO_2 reached to 8 wt.%, the amount of β-spodumene was highest at 880 °C. By contrasting Fig. 2 and Fig. 3, it indicated CeO_2 could accelerate crystals growth in LZS system, and it is more obvious at higher temperature. Table 3 shows more details of crystalline phase changes of the samples containing different content of CeO_2.

The microstructures of the samples are showed in Fig. 4 and 5. The chosen scanning electron microscope pictures were representative, which were C_0, C_2, C_6, C_8 heat-treated at 700 °C and 880 °C for 2 h, respectively. The morphology in Fig. 4(a) and (b) was similar. The interconnected network microstructure formed by tiny dendritic crystals, and the crystals in picture (b) was much bolder. According to the XRD analysis, the main crystals in Fig. 4(a) and (b) were Li_2ZnSiO_4 and $Li_3Zn_{0.5}SiO_4$ at 700 °C. The microstructures of glass-ceramics had changed significantly when CeO_2 content were 6 and 8 wt.%, showing in Fig. 4(c) and (d). A lot of β-spodumene crystals formed. The morphologies become smaller network-shaped microstructure, and crystals density increased. The development and disorderly distribution of massive thin small dendritic crystals resulted in the formation of honeycomb-shaped network structure. As the amount of CeO_2 increasing, the dendritic crystals became coarser, as shown in Fig. 4(d).

When the heat-treated temperature was 880 °C, the effect of CeO_2 on the crystals was more obvious. The microstructures of CeO_2-free sample appeared different parts (Fig. 5(a)). The spherical crystals could be observed, which was cristobalite crystal. Contrasting with Fig. 4(d), Fig. 5(b) had similar crystalline structure with it. It showed that CeO_2 would have a much stronger impact on promoting crystals formation at a high temperature (880 °C). The Fig. 5(c) has a looser net-work structure than that of picture (b). The reason was that with the increasing of CeO_2, the effect of partial substitution of Si^{4+} by Al^{3+} ions became stronger [32] and caused crystallization and development of β-spodumene. The grain of cristobalite grew bigger, distributing in tiny

Table 3. Effect of CeO_2 and heat treatment on the formation of crystalline phase.

Heat treatment condition	Glass code	Crystalline phase
700 °C + 2 h	C_0	$Li_3Zn_{0.5}SiO_4$, Li_2ZnSiO_4, cristobalite
	C_2	$Li_3Zn_{0.5}SiO_4$, Li_2ZnSiO_4, cristobalite
	C_4	$Li_3Zn_{0.5}SiO_4$, Li_2ZnSiO_4, cristobalite
	C_6	$Li_3Zn_{0.5}SiO_4$, Li_2ZnSiO_4, β-spodumene, cristobalite
	C_8	$Li_3Zn_{0.5}SiO_4$, Li_2ZnSiO_4, β-spodumene, cristobalite
880 °C + 2 h	C_0	$Li_3Zn_{0.5}SiO_4$, Li_2ZnSiO_4, cristobalite
	C_2	$Li_3Zn_{0.5}SiO_4$, Li_2ZnSiO_4, β-spodumene, cristobalite
	C_4	$Li_3Zn_{0.5}SiO_4$, Li_2ZnSiO_4, β-spodumene, cristobalite
	C_6	$Li_3Zn_{0.5}SiO_4$, Li_2ZnSiO_4, β-spodumene, cristobalite
	C_8	$Li_3Zn_{0.5}SiO_4$, Li_2ZnSiO_4, β-spodumene, cristobalite

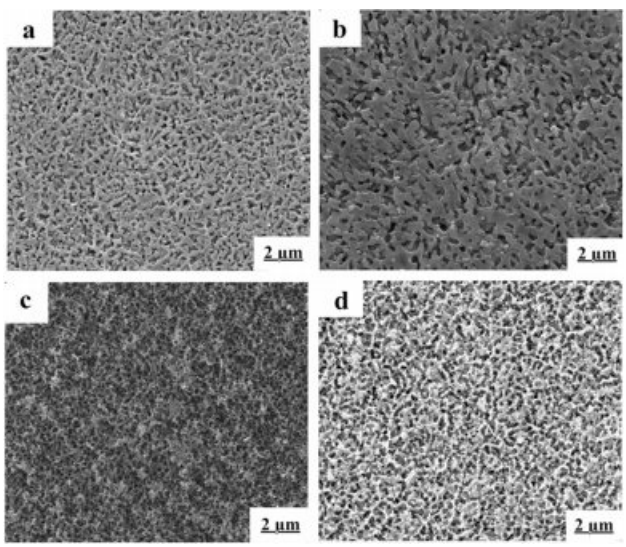

Fig. 4. Microstructure of the LZS glass-ceramics heat-treated at 700 °C for 2 h with different mounts of CeO_2: (a) 0 wt.%, (b) 2 wt.%, (c) 6 wt.%, (d) 8 wt.%.

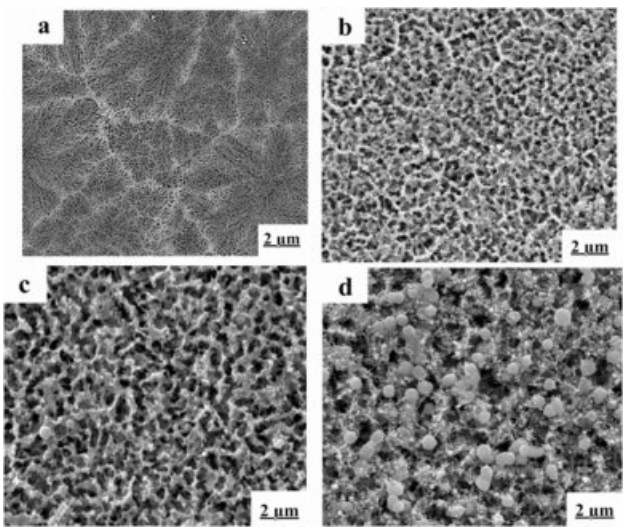

Fig. 5. Microstructure of the LZS glass-ceramics heat-treated at 880 °C for 2 h with different mounts of CeO_2: (a) 0 wt.%, (b) 2 wt.%, (c) 6 wt.%, (d) 8 wt.%.

dendritic β-spodumene crystals, which could be seen in Fig. 5(d).

Hardness (H_v) and Thermal expansion coefficient (α)

Vickers hardness of the glass-ceramics was an important property. The samples crystallized at 730 °C and 880 °C were tested, and the results were showed in Table 4. The microhardness of LZS glass-ceramics increased with CeO_2 increasing, as showing in Fig. 6. It was already pointed out that β-spodumene and cristobalite crystals increased in the glass-ceramics, which both have higher bond strength than $Li_3Zn_{0.5}SiO_4$ and Li_2ZnSiO_4 crystals. That was the reason of increase in hardness [33]. The hardness curves crystalized at 700 °C in Fig. 6 had biggest changes when the amount of CeO_2 was from 2 to 4 wt.%. However, at 880 °C, the changes happened when the amount of CeO_2 was from 0 to 2 wt.%. They were both reached to the maximums, 6.68 GPa and 6.88 GPa respectively, when CeO_2 content was 8 wt.%. It suggested high temperature could enhance the effect of CeO_2 in LZS glass-ceramics, which is similar with the XRD results. The increase of microhardness was in favour of advancing the sealing application of LZS glass-ceramics.

The LZS glasses are mainly used to seal to metals, and the thermo-physical property of the glasses is vital. The average thermal expansion coefficient at 20-450 °C was investigated. The results were showed in Table 4. Fig. 6 showed the change of thermal expansion coefficients at different crystallization temperatures versus CeO_2 content. The thermal expansion coefficients was first increasing then decreasing, as showing in Fig. 6, and reached to the maximums when the amount of CeO_2 was 4 wt.%. According to the XRD results in Fig. 2, when the amount of CeO_2 is free, the main crystals are Li_2ZnSiO_4 and $Li_3Zn_{0.5}SiO_4$, which have low thermal expansion coefficients ($\alpha \approx 110\times10^{-7}$ K^{-1}). However, the amount of cristobalite ($\alpha \approx 270\times10^{-7}$ K^{-1}) increased with CeO_2 increasing. The thermal expansion coefficient of LZS glass-ceramics increased, and reached to the maximum. With the amount of CeO_2 increasing (above 4 wt.%), it promoted the formation of β-spodumene, which has a lower thermal expansion coefficient ($\alpha \approx 19\times10^{-7}$ K^{-1}). The thermal expansion coefficient of LZS glass-ceramics decreased with β-spodumene increasing. When the crystallization temperature reached to 880 °C, the effect of CeO_2 promoting β-spodumene and cristobalite formation was more obvious, and β-spodumene crystals increased more apparently with CeO_2 content increasing. The glass-ceramics had lower thermal expansion coefficient when the amount of CeO_2 was above 6 wt.% at 880 °C. A small amount of CeO_2 (under 4 wt.%) could increase the average thermal expansion coefficients of LZS glass-ceramics, but it would markedly decrease when high CeO_2 content promoted the formation of β-spodumene. It could be concluded that LZS glass-ceramics could have a wide range of thermal expansion coefficients with the changes of temperature and CeO_2 content. The change of thermal expansion coefficient would make it better seal to more metals.

Table 4. The average thermal expansion coefficients at 20-400 °C and Vicker's hardness (± 0.02) of different amount of CeO_2-doped samples crystallized at 700 °C and 880 °C for 2 h.

Glass code	Crystallized at 700 °C/2 h		Crystallized at 880 °C/2 h	
	TEC ($\pm 2\times10^{-7}K^{-1}$)	H_v (GPa)	TEC ($\pm 2\times10^{-7}K^{-1}$)	H_v (GPa)
C_0	142	5.32	160	5.52
C_2	161	5.44	165	6.46
C_4	175	6.36	178	6.62
C_6	165	6.52	161	6.76
C_8	160	6.68	154	6.88

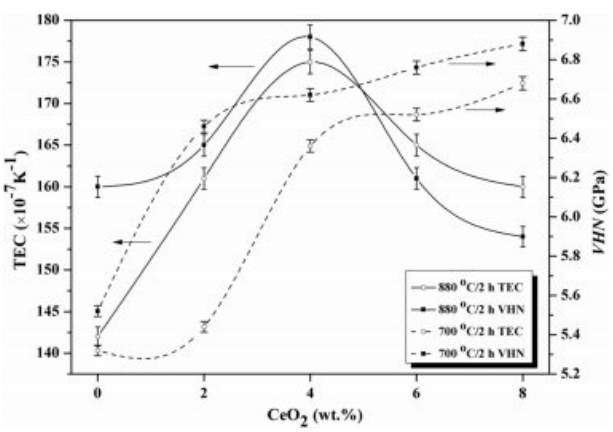

Fig. 6. Variation of microhardness and thermal expansion coefficients (TEC) with CeO_2 contents.

Conclusions

The amount of CeO_2 could affect the crystallization and thermo-physical properties of lithium zinc silicate glass-ceramics. The glass transition temperature (T_g) increased, but CeO_2 promoted the formation of β-spodumene and cristobalite crystals, which made the structure more rigid and caused the change of thermo-physical property, and the effects were more obvious at high crystallization temperature. The microhardness increased with CeO_2 content increasing; however, the average thermal expansion coefficients (20-450 °C) of LZS glass-ceramics showed first increasing then decreasing, and it obtained a wider range and reached to maximums when the amount of CeO_2 was 4 wt.%. The analysis indicated that CeO_2 played an important role in adjusted the crystallization and physical properties. And a higher microhardness and a wider average thermal expansion coefficient indicated the LZS glass-ceramics could better seal to metals.

Acknowledgment

The work was financially supported by Science and Technology Research Foundation of Jiangxi Education Department (No. GJJ170537/GJJ170498) and Startup Foundation for Docotors of Jiangxi University of Science and Technology (No. jxxjbs17019).

References

1. S.C. Clausbruch, M. Schweiger, W. Höland, and V. Rheinberger, J. Non-Cryst. Solids 263 (2000) 388-394.
2. B.I. Shaima and M. Goswami, J. Mater. Lett. 58 (2004) 2423-2438.
3. I.W. Donald, J. Non-cryst. solids (2004) 345-346.
4. M. Goswami, S.K. Deshpande, and R. Kumar, J. Phys. Chem. Solid. 71 (2010) 739-744.
5. W.Z. Liu, Z.W. Lou, X.L. Hu, and A.X. Lu, Thermochim. Acta. 584 (2014) 45-50.
6. Y.Z. Chen, W.H. Li, Y. Zhang, Z.Q. Shen, D.L. Yang, and X. Z. Song, Ceram. Int. 42 (2016) 11650-11653.
7. S.M. Salman, S.N. Salama, and H.A. Abo-Mosallam, Bol. Soc. Esp. Ceram. V. 56 (2017) 205-214.
8. P.W. McMillan and B.P. Hodgson, Glass Tech. 7 (1966) 121.
9. P.W. McMillan, G. Partridge, and B.P. Hodgson, Glass Tech. 7 (1966) 128.
10. I.W. Donald and B.L. Metcalfe, J. Mater. Sci. 24 (1989) 3892-3903.
11. I.W. Donald, P.M. Mallinson, and B.L. Metcalfe, J. Mater. Sci. 46 (2011) 1975-2000.
12. A. Karamanov, P. Pisciella, and M. Pelino, J. Eur. Ceram. Soc. 20 (2000) 2233-2237.
13. J.J. Shyu and M.T. Chiang, J. Am. Ceram. Soc. 83 (2000) 635-639.
14. A.W.A El-Shennawi, E.M.A. Hamzawy, and G.A. Khater, Ceram. Int. 27 (2001) 725-730.
15. W. Zheng, J. Cheng, and L. Tang, Thermochim. Acta 456 (2007) 69-74.
16. H.B. Zhang, G. Gui, C.H. Su, Y.M. Wang, and J. Shao, Chinese J. Inorg. Chem. 26 (2010) 144-148.
17. Y. Demirci and E. Günay, J. Ceram. Process. Res. 12 (2011) 352-356.
18. Z. Shen, Z. Liang, and Z. Yong, Ceram. Int. 43 (2017) 7099-7105.
19. D. Lee and S. Kang, J. Ceram. Process. Res. 19 (2018) 504-508.
20. G.P. Singh and D.P. Singh, Physica B 406 (2011) 640-644.
21. E. Mansour, J. Non-Cryst. Solids 357 (2011) 1364-1369.
22. P.S. Gurinder and D.P. Singh, Physica B 407 (2012) 4168-4172.
23. H.J. Wang, B.T. Li, and H.X. Lin, Int. J. Appl. Glass Sci. 7 (2016) 310-318.
24. H.J. Wang, B.T. Li, and H.X. Lin, J. Mater Sci-Mater. El. 27 (2016) 2860-2865.
25. T. Liu and G. Chen, Ceram. Int. 39 (2013) 5553-5559.
26. F. Soleimani and M. Rezvani, Mater. Res. Bull. 47 (2012) 1362-1367.
27. S.A.M. Abdel-Hameed and F.H. Margha, J. Alloys Compd. 554 (2013) 371-377.
28. S.B. Sohn, S.Y. Choi, and Y.K. Lee, J. Mater. Sci. 35 (2000) 4815-4821.
29. A.M. Hu, K.M. Liang, and F. Zhou, Ceram. Int. 31 (2005) 11-14.
30. J. Temuujin, U. Bayarzul, E. Surenjav, K. D. Sung, and C. Y. Sik, J. Ceram. Process. Res. 18 (2017) 112-115.
31. Y. S. Du, J. Ma, X. F. Zhang, H. X. Zhang, H. Chen, S. Ouyang, and B.W. Li, J. Ceram. Process. Res. 20 (2019) 401-410.
32. M. Goswami and P. Sengupta, Ceram. Int. 33 (2007) 863-867.
33. A.X. Lu and Z.B. Ke, J. Non-cryst. Solids 353 (2007) 2692-2697.
34. J. Zarzycki, in "Material Science and Technology" (Weinheim press, 1991) p667-713.